

Metastability and anomalous fixation in evolutionary games on scale-free networks

Michael Assaf*¹ and Mauro Mobilia*²

¹*Loomis Laboratory of Physics, Department of Physics 1110 West Green Street, Urbana, Illinois 61801, U.S.A*

²*Department of Applied Mathematics, School of Mathematics, University of Leeds, Leeds LS2 9JT, U.K.*

We study the influence of complex graphs on the metastability and fixation properties of a set of evolutionary processes. In the framework of evolutionary game theory, where the fitness and selection are frequency-dependent and vary with the population composition, we analyze the dynamics of snowdrift games (characterized by a metastable coexistence state) on scale-free networks. Using an effective diffusion theory in the weak selection limit, we demonstrate how the scale-free structure affects the system's metastable state and leads to *anomalous fixation*. In particular, we analytically and numerically show that the probability and mean time of fixation are characterized by stretched exponential behaviors with exponents depending on the network's degree distribution.

PACS numbers: 05.40.-a, 02.50.Ey, 87.23.Kg, 64.60.aq

The evolutionary dynamics of systems where successful traits spread at the expense of others is naturally modeled in the framework of evolutionary game theory (EGT) [1, 2]. In EGT, each species reproductive potential (fitness) varies with the population's composition and changes continuously in time. The selection is therefore “frequency-dependent” and the dynamics is traditionally studied in terms of differential equations [1–3]. Evolutionary dynamics is known to be affected by demographic noise and by the population's spatial arrangement [4, 5], and is often characterized by the central notion of fixation. This refers to the possibility that a “mutant type” takes over [6], and one is particularly interested in the *fixation probability* – the probability that a given trait invades an entire population, and in the *mean fixation time* (MFT) – the mean time for this event to occur. In contrast to what happens in spatially-homogeneous (well-mixed) populations, the spatial arrangement of individuals can give rise to very different scenarios [1, 4]. Evolutionary dynamics on networks [7] provides a general and unifying framework to describe the dynamics of both well-mixed and spatially-structured populations [8, 9]. In spite of its importance, fixation of evolutionary processes on networks has been mostly studied in idealized situations, *e.g.* for two-state systems under a constant weak selective bias [8–12]. In these works, it has been shown that the update rules and the network structure effectively renormalize the population size and thereby affect the fixation properties. Furthermore, some properties of evolutionary games have been studied on scale-free networks by numerical simulations, see *e.g.* [13], and on regular graphs with mean field and perturbative treatments [14]. The models of Refs. [9–12] are of great interest but do *not* provide a general description of evolutionary dynamics on graphs. In particular, these references consider constant fitness and selection pressure,

and thus can *not* describe systems possessing a long-lived *metastable* coexistence state prior to fixation [15, 16].

In this Letter we study metastability, which may arise as a consequence of frequency-dependent selection [3], and fixation on a class of scale-free networks in the EGT framework. To the best of our knowledge, such an analytical study has not been conducted before. For concreteness, we investigate “snowdrift games” (SGs, see below) [1, 16] that are the paradigmatic EGT models exhibiting metastability (see [17] for their experimental relevance). Our findings are also directly relevant to various fields, *e.g.* to population genetics [18] and to the dynamics of epidemic outbreaks, for which a long-lived endemic state is often an intrinsic characteristic [15, 19, 20].

For well-mixed populations (complete graphs) the fixation properties of SGs typically exhibit an exponential dependence on the population size, see *e.g.* [16]. Our central result is the demonstration that evolutionary dynamics on scale-free networks can lead to *anomalous* fixation and metastability characterized by a stretched exponential dependence on the population size, in stark contrast with their non-spatial counterparts. In the same vein as in [11], the analytical description is based on an effective diffusion theory derived from an individual-based formulation of the dynamics.

The model. We consider a network comprising N nodes, each of which is either occupied by an individual of type C (cooperator) or by a D-individual (defector). The occupancy of the node i is encoded by the random variable η_i , with $\eta_i = 1$ if the node i is occupied by a C and $\eta_i = 0$ otherwise. The state of the system is thus described by $\{\boldsymbol{\eta}\} = \{\eta_i\}^N$ and the density of cooperators present in the system is $\rho \equiv \sum_{i=1}^N \eta_i / N$. The network is specified by its adjacency matrix $\mathbf{A} = [A_{ij}]$, whose elements are 1 if the nodes ij are connected and 0 otherwise. The network is also characterized by its degree distribution $n_k = N_k / N$, where N_k is the number of nodes of degree k . EGT is traditionally concerned with large and homogeneous populations (i.e. $N \rightarrow \infty$ and $A_{ij} = 1, \forall ij$) whose mean field dynamics

*The authors contributed equally to this work.

is described by the celebrated replicator equation [1, 2]: $(d/dt)\rho(t) = \rho(t)(1 - \rho(t))[\Pi^C(\rho(t)) - \Pi^D(\rho(t))]$, where $\Pi^{C/D}(\rho(t))$ are the cooperator/defector average payoffs derived from the game's payoff matrix. For a generic two-strategy cooperation dilemma, the payoff of C against another C is denoted a and that of D playing against D is d . When C plays against D the former gets payoff b and the latter gets c [1]. Here we focus on SGs, for which $c > a$ and $b > d$. SGs are characterized by a stable interior fixed point $\rho_* = (d - b)/(a - b - c + d)$ and unstable absorbing states $\rho = 0$ (all-D) and $\rho = 1$ (all-C). For a finite population size ($N < \infty$) the role of fluctuations is important and ρ_* becomes a *metastable* state whose decay time on complete graphs ($A_{ij} = 1, \forall ij$) grows exponentially with N [16].

In a spatial setting, the interactions are among nearest-neighbor individuals and the species payoffs are defined locally: C and D players at node i interacting with a neighbor at node j respectively receive payoffs $\Pi_{ij}^C = a\eta_j + b(1 - \eta_j)$ and $\Pi_{ij}^D = c\eta_j + d(1 - \eta_j)$. In the spirit of the Moran model (in the weak selection limit) [2, 5, 6], each species local reproductive potential, or fitness, is given by the difference of $\Pi_{ij}^{C/D}$ relative to the population mean payoff $\bar{\Pi}_{ij}(t)$. Here, we make the mean-field-like choice $\bar{\Pi}_{ij}(t) = \rho(t)\Pi_{ij}^C + (1 - \rho(t))\Pi_{ij}^D$ to include what arguably is the simplest mechanism ensuring the formation of metastability. It is customary to introduce a selection strength $s > 0$ in the definition of the fitness to unravel the interplay between random fluctuations and selection [2, 5, 6]. Here, the fitnesses of C/D at node i interacting with a neighbor at node j are

$$f_{ij}^C = 1 + s[\Pi_{ij}^C - \bar{\Pi}_{ij}] \quad \text{and} \quad f_{ij}^D = 1 + s[\Pi_{ij}^D - \bar{\Pi}_{ij}]. \quad (1)$$

These expressions comprise a baseline contribution (set to 1) and a selection term proportional to the relative payoffs. Moreover, we consider a system evolving according to the so-called ‘‘link dynamics’’ (LD) [10, 11]: a link is randomly selected at each time step and if it connects a CD pair, one of the neighbors is randomly selected for reproduction with a rate proportional to its fitness, while the other is replaced by the offspring. While various types of update rules are possible [21], we here use the LD to highlight the combined effects of the topology and frequency-dependent selection: here, in stark contrast to the LD in the constant selection/fitness scenario [11], we show that the fixation properties strongly depend on the network's heterogeneity. Moreover, we have checked that our conclusion is robust and holds for various other update rules leading to metastability [22].

The evolution of the population's composition is described in terms of $\{\rho_k\}$, where $\rho_k = \sum_i \eta_i / N_k$ is the average number of cooperators on all nodes of degree k (the prime denotes summation over degree k nodes), i.e. ρ_k is the subgraph density of C's on nodes of degree k . Quantities necessary for our analysis are the m^{th} moment

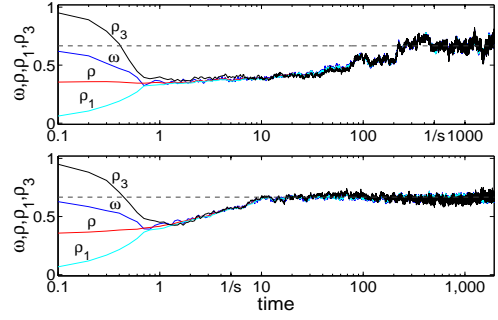


FIG. 1: (Color online). Timescale separation in the evolution of the densities ρ , ω , ρ_1 , and ρ_3 on a scale-free network with $\nu = 3$ for a SG with $a = d = 1, b = 9, c = 5$ and $N = 10^4$, see text. Numerical results for typical single-realization trajectories for $s = 0.002$ (top) and $s = 0.2$ (bottom). In both panels, initially $\rho_{k > \mu_1}(0) = 1, \rho_{k \leq \mu_1}(0) = 0$. As eye guides, the dashed line $\rho_* = 2/3$ and the times $t = s^{-1}$ are shown.

of the degree distribution, $\mu_m \equiv \sum_k k^m n_k = \sum_i k_i^m / N$, where k_i denotes the degree of node i , and the degree-weighted density of cooperators $\omega \equiv \sum_k (k/\mu_1) n_k \rho_k$.

Effective diffusion theory. To implement the evolutionary dynamics, we introduce $\Psi_{ij} = (1 - \eta_i)\eta_j f_{ji}^C$ and $\Psi_{ji} = (1 - \eta_j)\eta_i f_{ji}^D$, where $\eta_i(1 - \eta_j)$ is non-zero only when the nodes ij are occupied by a CD pair. In the LD, the probability to select the neighbor j of node i for an update is $A_{ij}/(N\mu_1)$ and the transition $\eta_i \rightarrow 1 - \eta_i$ hence occurs with probability $\sum_j \frac{A_{ij}}{N\mu_1} [\Psi_{ij} + \Psi_{ji}]$ [11]. The subgraph density ρ_k changes by $\pm \delta\rho_k = \pm 1/N_k$ according to a birth-death process [23] defined by the transition rates $T^+(\rho_k) = \sum_i \sum_j A_{ij} \Psi_{ij} / (N\mu_1)$ and $T^-(\rho_k) = \sum_i \sum_j A_{ij} \Psi_{ji} / (N\mu_1)$, respectively. For our analytical treatment, we focused on degree-heterogeneous networks with degree-uncorrelated nodes, as in Molloy-Reed networks (MRN) [24], yielding $A_{ij} = k_i k_j / (N\mu_1)$. Our numerical simulations were performed using the ‘‘redirection algorithm’’ that generates degree-correlated scale-free networks [25]. Yet, it has been shown that the dynamics on the latter is close to that on MRN [11]. With $\sum_i N^{-1} = n_k \rho_k$, the transition rates become

$$T^+(\rho_k) \equiv T_k^+ = (n_k/\mu_1) [1 + s(b - d)(1 - \rho)] k(1 - \rho_k)\omega$$

$$T^-(\rho_k) \equiv T_k^- = (n_k/\mu_1) [1 - s(a - c)\rho] k\rho_k(1 - \omega). \quad (2)$$

We notice that T_k^\pm are nonzero provided that the mean degree μ_1 does not diverge with $N \rightarrow \infty$ [26]. In the limit of weak selection intensity ($s \ll 1$), one can use the diffusion theory to treat the birth-death process defined by (2) [16]. This yields a multivariate backward Fokker-Planck equation (FPE) whose generator reads

$$\mathcal{G}(\{\rho_k\}) = \sum_k \left[\frac{(T_k^+ - T_k^-)}{n_k} \frac{\partial}{\partial \rho_k} + \frac{(T_k^+ + T_k^-)}{2Nn_k^2} \frac{\partial^2}{\partial \rho_k^2} \right], \quad (3)$$

with time increments $\delta t = N^{-1}$ [6, 23]. Furthermore, in the weak selection limit ($s \ll 1$), the analysis can be simplified using a timescale separation [11, 12] (see also [8]). When $t \ll s^{-1}$ the selection pressure is negligible and ρ is conserved [10]. In fact, using (2) at mean field level gives $(d/dt)\bar{\rho} = s(a - b - c + d)\bar{\omega}(1 - \bar{\omega})(\bar{\rho} - \rho_*)$ [the upper bar denotes the ensemble average]. This indicates that $\bar{\rho}$ relaxes to its metastable value ρ_* on a timescale $t \sim s^{-1} \gg 1$, see Fig. 1. At mean field level, Eqs. (2) also yield $(d/dt)\bar{\rho}_k = (T_k^+(\bar{\rho}_k) - T_k^-(\bar{\rho}_k))/n_k = (k/\mu_1) \times \{\bar{\omega} - \bar{\rho}_k + s[(b-d)\bar{\omega}(1-\bar{\rho})(1-\bar{\rho}_k) + (a-c)(1-\bar{\omega})\bar{\rho}_k\bar{\rho}]\}$. This indicates that after a timescale of order $\mathcal{O}(1)$, $\bar{\rho}_k \approx \bar{\omega}$, and also $\bar{\rho} \approx \bar{\omega}$ since $\bar{\rho} = \sum_k \bar{\rho}_k n_k$. With $\bar{\rho}_k \approx \bar{\omega} \approx \bar{\rho}$, the rate equation for $\bar{\rho}_k$ becomes $(d/dt)\bar{\rho}_k \simeq -(k/\mu_1)(b-d)s(1-\bar{\rho}_k)\bar{\rho}_k(\bar{\rho}_k/\rho_* - 1)$. Hence, while after a time of order $\mathcal{O}(1)$, $\bar{\rho}_k \approx \bar{\omega} \approx \bar{\rho}$, all these quantities slowly approach ρ_* after a time $t \sim s^{-1}$. This is illustrated in Fig. 1 where all trajectories rapidly coincide and then attain ρ_* when $t \sim s^{-1}$. As fixation occurs on much longer timescales than s^{-1} , we approximate that on average $\rho_k \approx \rho \approx \omega$ in the same vein as in [11]. With the definition of ω , yielding $\partial_{\rho_k} \rightarrow (kn_k/\mu_1)\partial_\omega$, and the change of variables $\rho_k \rightarrow \omega$, Eq. (3) becomes the *effective single-coordinate* FPE generator:

$$\mathcal{G}_{\text{eff}}(\omega) = \frac{\omega(1-\omega)}{N_{\text{eff}}} \left[-\sigma(\omega - \rho_*) \frac{\partial}{\partial \omega} + \frac{1}{2} \frac{\partial^2}{\partial \omega^2} \right]. \quad (4)$$

The drift term is proportional to $\sigma \equiv 2(b-d)N_{\text{eff}}s_{\text{eff}}/\rho_*$, where the effective population size and selection intensity are $N_{\text{eff}} \equiv N(\mu_1)^3/\mu_3$ and $s_{\text{eff}} \equiv s\mu_2/(\mu_1)^2$. For scale-free networks with degree distribution $n_k \propto k^{-\nu}$ and finite average degree (i.e. $\nu > 2$) [26], the maximum degree is $k_{\text{max}} \sim N^{1/(\nu-1)}$ [27]. We thus obtain the moments μ_m [11] that yield the scaling of σ and $\sigma_{\text{re}} \equiv N_{\text{eff}}s_{\text{eff}}$:

$$\sigma \propto \sigma_{\text{re}} = sN \frac{\mu_1 \mu_2}{\mu_3} \sim \begin{cases} sN, & \nu > 4 \\ sN/\ln N, & \nu = 4 \\ sN^{(2\nu-5)/(\nu-1)}, & 3 < \nu < 4 \\ s\sqrt{N} \ln N, & \nu = 3 \\ sN^{(\nu-2)/(\nu-1)}, & 2 < \nu < 3. \end{cases} \quad (5)$$

To understand this nontrivial scaling, we focus on scale-free graphs with $2 < \nu < 3$ characterized by the divergence of μ_2 and μ_3 (when $N \rightarrow \infty$). Such networks comprise nodes of high degree (hubs) causing the reduction of the system's effective size, $N_{\text{eff}} \sim N^{(2\nu-5)/(\nu-1)} \ll N$, and of the system's relaxation time $t \sim s_{\text{eff}}^{-1}$ to ρ_* , with $s_{\text{eff}} \sim sN^{(3-\nu)/(\nu-1)} \gg s$. As a result, the fluctuations intensity ($\propto N_{\text{eff}}^{-1/2}$) and the drift strength ($\propto s_{\text{eff}}$) are both enhanced by the topology. Yet, their product $N_{\text{eff}}s_{\text{eff}} \sim sN^{(\nu-2)/(\nu-1)} \ll Ns$ indicates that their combined effect drastically reduces the MFT (see below). We have also checked that our effective theory (4) is applicable when $s_{\text{eff}}^2 \ll N_{\text{eff}}^{-1}$, i.e. over a broader range of s than on complete graphs when $2 < \nu < 4$ [28].

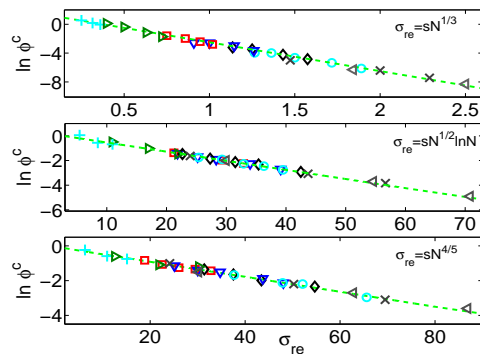


FIG. 2: (*Color online*). Probability ϕ^C versus σ_{re} for SGs with $a = d = 1$, $b = 1.05$, $c = 1.075$ and $s = 0.025$ (+), 0.05 (\triangleright), 0.075 (\square), 0.1 (∇), 0.125 (\diamond), 0.15 (\circ), 0.2 (\times), 0.25 (\triangleleft). Numerical results for $\nu = 2.5$ (top), $\nu = 3$ (middle), $\nu = 3.5$ (bottom) collapse along the straight dashed lines obtained from (6), see text. Here $N = 400 - 4000$ and initially $\rho_k = \rho = \omega = 100/N$. Error bars are of size of the symbols.

Fixation properties. Evolutionary dynamics is characterized by the fixation probability $\phi^C(\omega)$ that a system with initial degree-weighted density ω is taken over by cooperators. In the framework of the effective diffusion theory and using (4) the fixation probability obeys $\mathcal{G}_{\text{eff}}(\omega)\phi^C(\omega) = 0$ with boundary conditions (BCs) $\phi^C(0) = 1 - \phi^C(1) = 0$ [5, 23]. The solution reads

$$\phi^C(\omega) = \frac{\text{erfi}[\rho_*\sqrt{\sigma}] - \text{erfi}[(\rho_* - \omega)\sqrt{\sigma}]}{\text{erfi}[\rho_*\sqrt{\sigma}] + \text{erfi}[(1 - \rho_*)\sqrt{\sigma}]}, \quad (6)$$

where $\text{erfi}(z) \equiv \frac{2}{\sqrt{\pi}} \int_0^z e^{u^2} du$. Let us consider the (biologically relevant) case of a small initial density of cooperators such that $\omega \ll 1$, weak selection [5, 6], and a large population such that $\rho_*^2\sigma \gg 1$ and metastability is guaranteed. Using the asymptote $\text{erfi}(x) \sim e^{x^2}$ for $x \gg 1$ in Eq. (6), we distinguish two cases: (i) when $\rho_* < 1/2$, $\ln \phi^C \simeq -(1 - 2\rho_*)\sigma$; (ii) when $\rho_* > 1/2$ and $\omega > 2\rho_* - 1$, $\ln(1 - \phi^C) \simeq -(2\rho_* - 1)\sigma$, while $\ln(1 - \phi^C) \simeq -\omega(2\rho_* - \omega)\sigma$ if $\rho_* > 1/2$ and $\omega < 2\rho_* - 1$. In Fig. 2 (and Fig. 3), for each value of s the numerical results have been rescaled by a constant to test the scaling (5). The linear data collapse and stretched exponential dependence $\ln \phi^C \sim -sN\mu_1\mu_2/\mu_3$ predicted by (5,6) is indeed clearly observed in Fig. 2. Since $\ln \phi^C \sim -sN$ on complete graphs [16], this demonstrates how the scale-free structure drastically affects the fixation probability.

Another quantity of great interest is the (unconditional) MFT $\tau(\omega)$ – the mean time necessary to reach an absorbing boundary. Here, using Eq. (4) the MFT is obtained by solving $\mathcal{G}_{\text{eff}}(\omega)\tau(\omega) = -1$ with BCs $\tau(0) = \tau(1) = 0$ [23]. Using standard methods [6, 23], we obtain $\tau(\omega) = 2N_{\text{eff}} \left[(1 - \phi^C(\omega)) \int_0^\omega dy \frac{e^{-\Theta(y)}}{y(1-y)} \int_0^y dz e^{\Theta(z)} + \phi^C(\omega) \int_\omega^1 dy \frac{e^{-\Theta(y)}}{y(1-y)} \int_y^1 dz e^{\Theta(z)} \right]$; $\Theta(z) \equiv \sigma z(z - 2\rho_*)$. For $\rho_*^2\sigma \gg 1$ the inner integrals can be computed by expand-

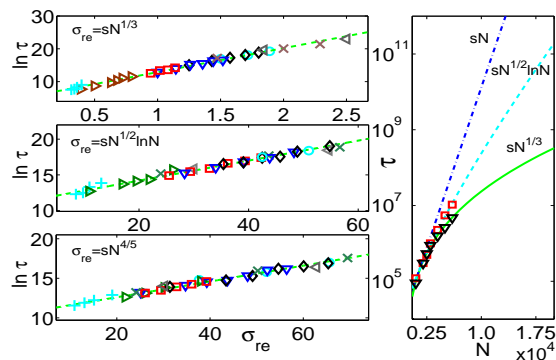


FIG. 3: (Color online). (Left) τ vs σ_{re} for $\nu = 2.5$ (top), $\nu = 3$ (middle), and $\nu = 3.5$ (bottom). Numerical results (symbols) collapse along lines (dashed) in agreement with (7), see text. Symbols and parameters are as in Fig. 2. (Right) τ vs N on semi-log scale with $s = 0.1$: numerical results for $\nu = 2.5$ (∇) and $\nu = 3$ (\square) agree with (7), shown as solid/dashed lines. The result on complete graphs ($\ln \tau \sim sN$) is sketched as eye guide (dash-dotted). In all panels, initially $\rho_k = \rho = 0.5$.

ing $\Theta(z)$ around its extremal values ($z = 0$ for $z \in [0, \rho_*]$ and $z = 1$ for $z \in [\rho_*, 1]$), while the outer integral is computed via the saddle-point approximation around $\omega = \rho_*$. To leading order, one thus obtains a stretched exponential dependence on N : $\tau(\omega) \sim (1 - \phi^C(\omega))e^{\sigma\rho_*^2}$ when $\omega > \rho_*$ and $\tau(\omega) \sim \phi^C(\omega)e^{\sigma(1-\rho_*)^2}$ otherwise. For example, when $\rho_* < 1/2$ this gives (see Fig. 3)

$$\ln \tau(\omega) \simeq \sigma\rho_*^2 \propto \sigma_{re}. \quad (7)$$

When the initial number of cooperators is not too low, the long-lived metastable state is entered prior to fixation and the MFT (7) is independent of the initial condition [15, 16]. Eq. (7), confirmed by Fig. 3, implies that for scale-free networks with $2 < \nu < 4$ fixation occurs much more rapidly than on complete graphs, a phenomenon called “hyperfixation” in genetics [18].

Discussion & conclusion. We have studied metastability and fixation of evolutionary processes on scale-free networks in the realm of EGT. For the sake of concreteness, we have focused on “snowdrift games” evolving with the LD [11] and characterized by a long-lived (metastable) coexistence state. The evolutionary dynamics has been described by a birth-death process from which we have derived an effective diffusion theory by exploiting a timescale separation occurring at weak selection intensity. The probability and mean fixation time (MFT) have been computed from the corresponding backward Fokker-Planck equation. These quantities exhibit a stretched-exponential dependence on the population size, in stark contrast with their non-spatial counterparts. We have checked with various update rules that the stretched-exponential behavior is a generic feature of metastability on scale-free graphs that also characterizes the fixation probability of coordina-

tion games [1, 22]. Here, important consequences of the stretched-exponential behavior are a drastic reduction of the MFT and the possible enhancement of the fixation probability of a few mutants with respect to a non-spatial setting. These anomalous fixation and metastability properties reflect the strong influence of the network’s structure on evolutionary processes.

-
- [1] J. Maynard Smith, *Evolution and the Theory of Games* (Cambridge University Press, Cambridge, 1982); J. Hofbauer and K. Sigmund, *Evolutionary Games and Population Dynamics* (Cambridge University Press, Cambridge, 1998); G. Szabó and G. Fáth, *Phys. Rep.* **446**, 97 (2007).
 - [2] M. A. Nowak, *Evolutionary Dynamics* (Belknap Press, 2006).
 - [3] P. Taylor and L. Jonker, *Math. Biosci.* **40**, 145 (1978); J. Hofbauer *et al.*, *J. Theo. Bio.* **81**, 609 (1979).
 - [4] M. A. Nowak and R. M. May, *Nature* **359**, 826 (1992); C. Hauert and M. Doebeli, *Nature* **428**, 643 (2004); M. Nowak, *Science* **314**, 1560 (2006); A. Traulsen *et al.*, *Proc. Nat. Acad. Sci. USA* **107**, 2962 (2010).
 - [5] M. A. Nowak *et al.*, *Nature* **428**, 646 (2004); A. Traulsen *et al.*, *Phys. Rev. E* **74**, 021905 (2006); B. Wu *et al.*, *Phys. Rev. E* **82**, 046106 (2010).
 - [6] J. F. Crow and M. Kimura, *An Introduction to Population Genetics Theory* (Blackburn Press, New Jersey, 2009); W. J. Ewens, *Mathematical Population Genetics* (Springer, New York, 2004).
 - [7] A. L. Barabási and R. Albert, *Science* **286**, 509 (1999); R. Albert and A. L. Barabási, *Rev. Mod. Phys.* **74**, 47 (2002); M. E. J. Newman, *SIAM Rev.* **45**, 167 (2003); P. Shakarian *et al.*, *BioSystems* **107**, 66 (2012).
 - [8] H. Ohtsuki *et al.*, *Nature* **441**, 502 (2006).
 - [9] E. Lieberman *et al.*, *Nature* **433**, 312 (2005).
 - [10] C. Castellano, D. Vilone, and A. Vespignani, *EPL* **63**, 153 (2003); K. Suchecki *et al.*, *EPL* **69**, 228 (2005).
 - [11] V. Sood and S. Redner, *Phys. Rev. Lett.* **94**, 178701 (2005); T. Antal *et al.*, *Phys. Rev. Lett.* **96**, 188104 (2006); V. Sood *et al.*, *Phys. Rev. E* **77**, 041121 (2008).
 - [12] G. J. Baxter *et al.*, *Phys. Rev. Lett.* **101**, 258701 (2008); R. A. Blythe, *J. Phys. A: Math. Theo.* **43**, 385003 (2010).
 - [13] F. C. Santos and J. M. Pacheco, *Phys. Rev. Lett.* **95**, 098104 (2005); F. C. Santos *et al.*, *Proc. Nat. Acad. Sci. USA* **103**, 3490 (2006).
 - [14] H. Ohtsuki and M. A. Nowak, *J. Theo. Bio.* **243**, 86 (2006); C. E. Tarnita *et al.*, *J. Theo. Bio.* **259**, 570 (2009).
 - [15] M. Assaf and B. Meerson, *Phys. Rev. Lett.* **97**, 200602 (2006); *Phys. Rev. E* **81**, 021116 (2010).
 - [16] M. Mobilia and M. Assaf, *EPL* **91**, 10002 (2010); M. Assaf and M. Mobilia, *J. Stat. Mech.*, **P09009** (2010).
 - [17] J. Gore *et al.*, *Nature* **459**, 253 (2009).
 - [18] P. A. Wigham *et al.*, *Th. Pop. Bio.* **74**, 283 (2008).
 - [19] R. Pastor-Satorras and A. Vespignani, *Phys. Rev. Lett.* **86**, 3200 (2001); R. M. May and A. L. Lloyd, *Phys. Rev. E* **64**, 066112 (2001); M. E. J. Newman, *Phys. Rev. E* **66**, 016128 (2002);
 - [20] I. Näsell, *J. Theo. Bio.* **211**, 11 (2001).
 - [21] One can also use the voter model or invasion process update rules. These and the LD are equivalent on regular

- graphs, but markedly different on scale-free graphs [11].
- [22] M. Assaf and M. Mobilia, in preparation.
 - [23] C. W. Gardiner, *Handbook of Stochastic Methods*, (Springer, New York, 2002).
 - [24] M. Molloy and B. Reed, *Random. Struct. Algorithms* **6**, 161 (1995).
 - [25] S. N. Dorogovtsev *et al.*, *Phys. Rev. Lett.* **85**, 4633 (2000); P. L. Krapivsky and S. Redner, *Phys. Rev. E* **63**, 066123 (2001).
 - [26] Our model does not apply to (unrealistic) graphs with $\nu \leq 2$, i.e. with diverging average degree μ_1 , see Eqs. (2).
 - [27] P. L. Krapivsky and S. Redner, *J. Phys. A* **35**, 9517 (2002).
 - [28] E.g., (4) is valid for $s^2 \ll N^{-1/(\nu-1)}$ when $2 < \nu < 3$, while the condition on complete graphs is $s^2 \ll N^{-1}$ [16].